Stationary Population Inversion in an Expanding Argon Plasma Jet by Helium Puffing

H. Akatsuka* and K. Kano*

*Research Laboratory for Nuclear Reactors, Tokyo Institute of Technology, 2-12-1-N1-10, O-Okayama, Meguro-ku, Tokyo, 152-8550, Japan

Abstract. An experiment of He gas-contact for generating population inversion in a recombining Ar plasma jet is carried out. Population inversion between Ar I excited states $5s' \rightarrow 4p'[1/2]_1$ and $5s' \rightarrow 4p[3/2]_{1,2}, [5/2]_{2,3}$ is created by helium gas-contact cooling of electrons, whereas it is not created without gas-contact. Ar I lines 1.14 μm, 1.34 μm, and 1.09 μm are strongly enhnced due to the He gas cooling. It is experimentally found that helium gas contact effectively lowers electron temperature of the Ar plasma jet. The mechanisms giving rise to population inversion are discussed in terms of atomic collisional processes of the recombining plasma. The experimental results of electron temperature and population densities are discussed by simple numerical analysis which we previously developed. It is shown that the experimental results are well explained by our modeling quantitatively for the case without gas contact, except that the agreement of number densities of lower lying non-LTE levels is qualitative for the case with the gas contact.

INTRODUCTION

The authors have been studying fundamental spectroscopic characteristics of hydrogen and noble gas plasmas generated by a plasma jet apparatus [1]. These plasmas are in a typical recombining phase, and stationary population inversions of H I and He I have been observed by spectroscopic examinations [2, 3, 4]. On the other hand, no population inversion of Ar I was observed for the argon plasma in the same discharge apparatus. Collisional radiative model theoretically showed that electron temperature should be sufficiently low in order to create population inversion in recombining plasmas [5]. We found that the electron temperature of the hydrogen and helium plasmas was about 0.1 eV or much lower and cold enough to make population inversion, whereas that of the argon plasma was about 0.5 eV, by spectroscopic measurement. It was supposed that electron gas in the downstream region of the plasma jet becomes relaxed mainly by collisions with residual gaseous molecules in the plasma jet chamber [4]. The authors consider that the result of the Ar plasma is attributed to the fact that the cross section of elastic collision between an electron and an argon atom is reduced owing to the Ramsauer effect in the energy range about $0.2 - 0.5$ eV [6]. And consequently, electron temperature of the argon plasma does not become lower than 0.5 eV, and no population inversion occurs, whereas electron temperature of hydrogen and helium plasmas was found to be as low as 0.1 eV due to frequent collisions of electrons with residual gaseous molecules in the plasma expansion region, since they have no Ramsauer minimum in their elastic electron scattering cross sections.

The authors have numerically investigated an effect of He gas-contact cooling of electrons on generation of population inversion in the Ar plasma [7]. It was shown that the electron temperature of the Ar plasma was significantly decreased by gas-contact cooling, so that the population inversion of Ar I excited states $5s' \rightarrow 4p'[1/2]_1$ and $5s' \rightarrow 4p[3/2]_{1,2}, [5/2]_{2,3}$ was created. The objective of the present study is to demonstrate the effectiveness of the gas-contact cooling of electrons and to generate population inversion of Ar I experimentally. Another objective is to investigate the mechanism of the electron energy transfer in the recombining plasma jet.

EXPERIMENTAL SETUP

Figure 1(a) shows the schematic view of the plasma jet apparatus [1]. The apparatus is composed of a plasma generator, six magnetic coils, traversing mechanism for moving the optical fiber terminal assembly for spectroscopic

CP762, *Rarefied Gas Dynamics: 24th International Symposium,* edited by M. Capitelli

Report Documentation Page

Form Approved
OMB No. 0704-0188

1. REPORT DATE	2. REPORT TYPE	3. DATES COVERED
13 JUL 2005	**N/A**	**-**

4. TITLE AND SUBTITLE	5a. CONTRACT NUMBER
Stationary Population Inversion in an Expanding Argon Plasma Jet by Helium Puffing	5b. GRANT NUMBER
	5c. PROGRAM ELEMENT NUMBER
6. AUTHOR(S)	5d. PROJECT NUMBER
	5e. TASK NUMBER
	5f. WORK UNIT NUMBER
7. PERFORMING ORGANIZATION NAME(S) AND ADDRESS(ES) **Research Laboratory for Nuclear Reactors, Tokyo Institute of Technology, 2-12-1-N1-10, O-Okayama, Meguro-ku, Tokyo, 152-8550, Japan**	8. PERFORMING ORGANIZATION REPORT NUMBER
9. SPONSORING/MONITORING AGENCY NAME(S) AND ADDRESS(ES)	10. SPONSOR/MONITOR'S ACRONYM(S)
	11. SPONSOR/MONITOR'S REPORT NUMBER(S)

12. DISTRIBUTION/AVAILABILITY STATEMENT
Approved for public release, distribution unlimited

13. SUPPLEMENTARY NOTES
See also ADM001792, International Symposium on Rarefied Gas Dynamics (24th) Held in Monopoli (Bari), Italy on 10-16 July 2004.

14. ABSTRACT

15. SUBJECT TERMS

16. SECURITY CLASSIFICATION OF:			17. LIMITATION OF ABSTRACT	18. NUMBER OF PAGES	19a. NAME OF RESPONSIBLE PERSON
a. REPORT	b. ABSTRACT	c. THIS PAGE			
unclassified	**unclassified**	**unclassified**	**UU**	**6**	

Standard Form 298 (Rev. 8-98)
Prescribed by ANSI Std Z39-18

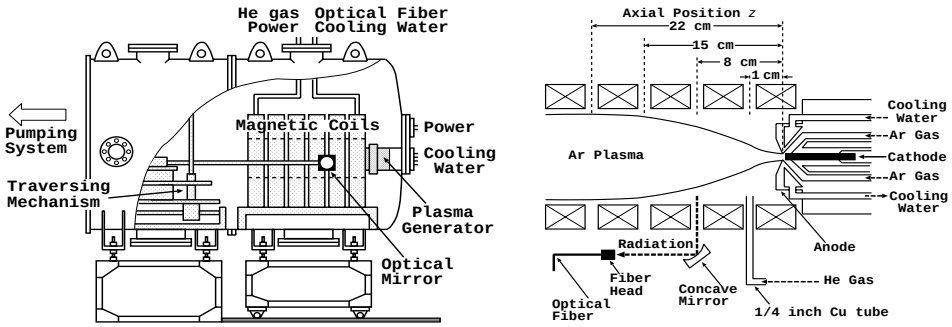

FIGURE 1. Cross-sectional view of (a) a plasma jet apparatus, and (b) electrodes, magnets and expanding plasma.

examinations. These components are placed in a wind tunnel of 1.2 m in diameter and 2 m in length. The pressure in the wind tunnel is monitored by a Pirani gauge. The wind tunnel is evacuated with a 12 inch mechanical booster pump, where the ultimate pressure becomes as low as 0.40 Pa with its pumping rate $10\,\mathrm{m}^3/\mathrm{sec}$. Figure 1(b) shows the cross-sectional view of the electrodes for generating the plasma, and the expanding plasma through the nozzle. To specify the spatial position of the Ar plasma generated, the axial distance from the anode, z, is employed. The anode is made of copper, and has a nozzle of 1.2 mm diameter of a convergent throat shape. The cathode is made of a $2\ \%$ thoriated tungsten rod of 3 mm in diameter. The argon plasma is generated by a DC arc discharge between the electrodes, and it expands after emerging from the nozzle on the anode. In the wind tunnel, six magnetic coils of 80 mm inner diameter are placed for confining the expanding plasma, with each gap distance of 1 cm. The strength of the magnetic field longitudinal to the center axis of the wind tunnel is about 0.15 T.

Spectroscopic measurement was carried out for the plasma through the gaps between the magnetic coils at $z = 1$, 8, 15, and 22 cm. To compare the results obtained by the numerical simulation [7], population densities of the levels defined in a Collisional-Radiative(CR) model [8] were chosen to be measured. An optical fiber assembly was employed to guide the radiation from the plasma to a monochromator system (JASCO, SS-50). The visible and infrared lines from the monochromator were detected by a photo-multiplier tube (Hamamatsu, R374) and by a Ge photo-diode (Hamamatsu, B3033-02), respectively. The signals from the photo-multiplier tube or from the Ge photo-diode were recorded by a computer. The sensitivity of the detection system was calibrated with a standard halogen lamp (Ushio Electric Corporation, JPD100V500WCS) and a white standard reflectance plate for a diffuse reflector.

A typical discharge conditions is as follows: arc voltage V_{arc} 18 V, discharge current I_{arc} 120 A, pressure in the wind tunnel P_{t} without He injection 1.3 Pa.

As shown in Fig. 1(b), a stationary injection of neutral He gas into the Ar plasma is carried out at $z = 1$ cm in such a way that the Ar plasma is not perturbed. The pressure P_{t} when He gas is introduced is 5.5 Pa, which corresponds to the maximum He gas flow rate where the axial symmetry of the Ar plasma is not perturbed. The number density of He atom N_{g} at $z = 1$ cm was estimated from the conductance of the wind tunnel and from the capacity of the pumping system employed, on the assumption that the temperature of the injected He gas was 300 K, which showed N_{g} being 3.4×10^{15} cm^{-3}. Experiments have been carried out for two cases: (A) the Ar plasma without He gas contact ($N_{\mathrm{g}} = 0$ cm^{-3}, hereafter called case A), and (B) the Ar plasma with He gas-contact ($N_{\mathrm{g}} = 3.4 \times 10^{15}$ cm^{-3}, hereafter called case B).

RESULTS AND DISCUSSION

Electron Temperature

Electron temperature T_{e} was determined from population distributions of high-lying levels of the Boltzmann plots obtained by spectroscopic measurements, since it was already shown that these levels of recombining plasmas were in a state of PLTE (partially local thermodynamic equilibrium) [1, 2, 3, 4]. Because the emission is observed along the direction perpendicular to the axis of the plasma jet and the Abel inversion is not applied, electron temperature obtained by spectroscopic measurement approximately corresponds to mean value along the line of sight.

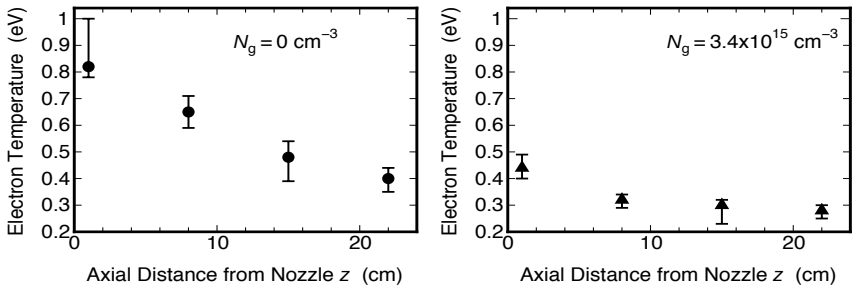

(a) case A (without gas-contact) (b) case B (with gas-contact)

FIGURE 2. Axial variation of electron temperature of (a) case A (without gas-contact) and (b)case B (with gas-contact).

Figures 2 (a) and (b) show axial variation of electron temperature of cases A and B, respectively. Electron temperature with gas-contact (case B) becomes as cold as 0.44 eV at $z = 1$ cm, while that without gas-contact (case A) remains 0.82 eV. This experimental result shows rapid cooling of electrons is accomplished by the helium gas-contact.

The decrease in $T_{\rm e}$ of case B from $z = 0$ to $z = 8$ cm becomes 0.48 eV, on the assumption that electron temperature of case B at $z = 0$ cm is close to that of case A at $z = 1$ cm, that is, 0.82 eV. On the other hand, the decrease in $T_{\rm e}$ of case B from $z = 8$ to $z = 22$ cm is reduced to 0.04 eV. This reduction of electron cooling can be explained on the basis of energy balance equation for electrons [9]. As we specify in the next chapter, electron temperature is temporally traced by the energy balance equation describing the energy increase of electrons per unit time [10]. The equation is expressed as

$$\frac{{\rm d}W_{\rm e}}{{\rm d}t} = R + Q, \tag{1}$$

where $W_{\rm e}$ is electron energy in a unit volume, i.e. $3N_{\rm e}k_{\rm B}T_{\rm e}/2$ ($k_{\rm B}$ being Boltzmann's constant, and $N_{\rm e}$ being electron density). The terms R and Q denote the energy transfer to free electrons due to elastic and inelastic collisions per unit time, respectively. And strictly speaking, concerning the term for elastic collisional processes, R, we should take the effect of electron-He atom collisions (e-He) $\varepsilon_{\rm He}$, electron-Ar collisions (e-Ar) $\varepsilon_{\rm Ar}$, and electron-Ar^+ (e-Ar^+) elastic collisions $\varepsilon_{\rm Ar^+}$ into account. In case B, the decrease in the electron energy is mainly attributed to the elastic collision processes between electrons and helium atoms $\varepsilon_{\rm He}$. The effect of inelastic scattering process is also negligible as we showed in our previous work [7]. Therefore, the electron energy loss of case B can be estimated by the following equation [11]

$$\frac{{\rm d}W_{\rm e}}{{\rm d}t} \simeq \varepsilon_{\rm He} = -\frac{2m_{\rm e}M_{\rm He}}{(m_{\rm e}+M_{\rm He})^2}\,\frac{3}{2}k_{\rm B}(T_{\rm e}-T_{\rm g})\,\langle\nu_{\rm He}\rangle\,N_{\rm e}, \tag{2}$$

where $m_{\rm e}$ and $M_{\rm He}$ are the mass of an electron and a He atom, respectively; $\langle\nu_{\rm He}\rangle$ is an effective collision frequency of electrons which collide with He atoms [12]; $T_{\rm g}$ is the He gas temperature. Since the collision frequency $\langle\nu_{\rm He}\rangle$ in Eq. (2) is proportional to the He atom density $N_{\rm g}$, rewriting Eq. (2) yields the simple expression

$$\frac{{\rm d}W_{\rm e}}{{\rm d}t} \simeq \varepsilon_{\rm He} \propto -(T_{\rm e}-T_{\rm g})N_{\rm g}. \tag{3}$$

This relationship shows that the energy transfer by the elastic collision of e-He is proportional both to the difference of the temperature $(T_{\rm e}-T_{\rm g})$ and to the density of He atom $N_{\rm g}$. In the range of $z \geq 8$ cm, electron temperature of case B decreases as such that the effect of e-He elastic collision on the cooling of electrons becomes small. This is because the term $(T_{\rm e}-T_{\rm g})$ in Eq. (3) becomes smaller as $T_{\rm e}$ becomes close to $T_{\rm g}$. Furthermore, because He atoms cannot be confined by the magnetic field and diffuse in the plasma chamber, the density of He atoms diminishes as the axial distance from the nozzle z increases. As a result, the effect of the gas-contact on electron cooling is reduced, thus variation of $T_{\rm e}$ dwindles for the range of $z \geq 8$ cm. In other words, this result also shows the electron energy transfer arises from the e-He elastic collision, particularly in the upstream region around $z \simeq 1$ cm, where the density of He gas is sufficiently high, since it is just introduced into the plasma at this position.

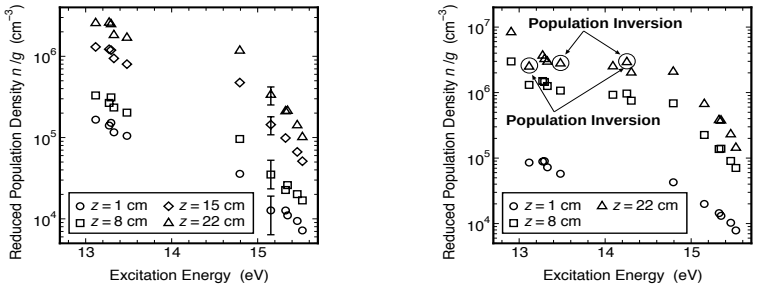

(a) case A (without gas-contact) (b) case B (with gas-contact)

FIGURE 3. Axial variation of reduced population density of (a) case A (without gas-contact) and (b) case B (with gas-contact).

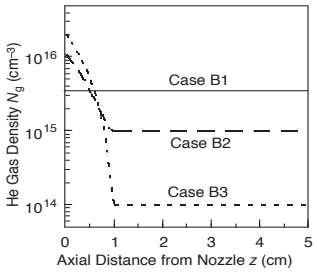

FIGURE 4. Helium number density profile assumed in Case B of the present simulation.

Population Density

Figures 3 (a) and (b) show axial variation of Boltzmann plots of Ar I for cases A and B, respectively. In Fig. 3 (b), since the population density at $z = 15$ cm is almost the same as that at $z = 22$ cm, the former is not presented. Besides, population densities of some levels are not shown for case A at any z or for case B at $z = 1$ cm, since the intensity of the corresponding line spectra in infrared region was too weak to observe.

It should be noted that population densities at $z = 8$ cm of case B are about 10 times higher than those of case A, which results from the difference in electron temperature of each case, namely, whether the He gas in introduced or not. In case B, population inversions between Ar I excited states of $5s' \rightarrow 4p'[1/2]_1$ $(i = 15 \rightarrow 11)$ and $5s' \rightarrow 4p[3/2]_{1,2}, [5/2]_{2,3}$ $(i = 15 \rightarrow 7)$ are observed. The corresponding overpopulation densities $\Delta(N/g)$ are 1.3×10^5 cm^{-3} and 4.3×10^5 cm^{-3}, respectively.

Discussion on the Experimental Results in terms of Simple Numerical Modeling

In order to discuss the present experimental results quantitatively, we employed our numerical modeling of gas contact cooling of the argon plasma jet [7].

A numerical simulation is carried out under the following assumptions: A quasi-neutral Ar plasma penetrates into a homogeneous and spatially-isotropic neutral He gas filled in the wind tunnel. The temperature of He gas T_g, is set to a fixed value, 300 K. Meanwhile, considering the present experimental conditions, we set N_g to 0 cm^{-3} for case A (without gas contact). For case B (with gas contact), it is quite difficult for us to measure the He number densities in the plasma expanding region experimentally. Therefore, to discuss the agreement of the numerical results with the present experimental ones, we assume three hypothetical He density profile $N_g(t)$ cm^{-3} as shown in Fig. 4.

In order to compare the numerical results with the present experimental ones, we need to know the longitudinal component of velocity of the plasma jet v_z, which was difficult for us to measure in the experiments. Here, we refer that of the hydrogen plasma jet in the present apparatus, which was measured from the Doppler shift of H_α line [2], where it was shown that v_z of the hydrogen plasma jet was about 1×10^6 cm/s. It was considered that the dissociation degree of hydrogen was almost unity due to the high initial gas temperature of the arc plasma jet. If we assume that

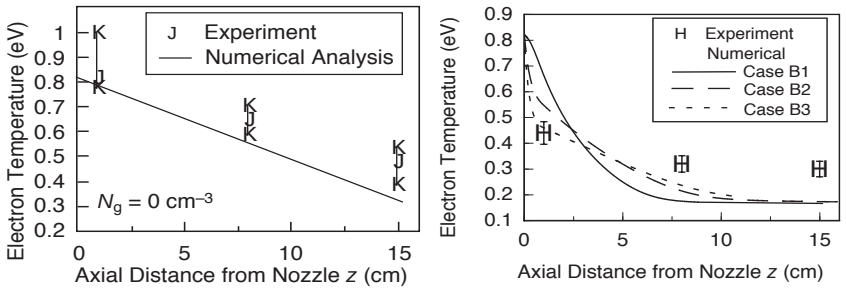

(a) case A (without gas-contact) (b) case B (with gas-contact)

FIGURE 5. Comparison of the electron temperature measured in the present experiments with that calculated by our simple numerical analysis. (a) case A (without gas-contact) and (b) case B (with the gas contact).

the Mach number of the argon plasma jet should be approximately equal to that of the hydrogen plasma jet, we can roughly estimate the longitudinal velocity of the argon plasma jet to be

$$\frac{v_z(\mathrm{Ar})}{v_z(\mathrm{H})} = \sqrt{\frac{\gamma(\mathrm{Ar})M_{\mathrm{H}}}{\gamma(\mathrm{H})M_{\mathrm{Ar}}}}, \tag{4}$$

where γ denotes the specific-heat ratio and M_{H} the mass of the hydrogen atom. In consequence, the value of v_z of the argon plasma jet is estimated at 1.6×10^5 cm/s. For a simple comparison, we also assume that the argon plasma drifts downstream at the uniform velocity 1.6×10^5 cm/s. This enables us to compare the experimental results with the calculation, by regarding that the longitudinal distance z corresponds to $v_z t$.

As a result, Figures 5 (a) and (b) show calculated values of T_{e} for case A (without the gas contact) and for cases B1, B2 and B3 (with the gas contact), respectively, together with their corresponding experimental results. It is found that the calculated electron temperature agrees well with our experimental results for case A. Although we made many assumptions in the course of our formulation, they are considered to be basically sufficient for quantitative numerical analysis for case A, namely, without gas-contact.

Concerning electron temperature for cases with gas contact, the agreement of the case B1 (constant density) is the poorest of the three. Of course, this is attributed to the unjustified assumption of the helium density profile. The helium density should become smaller as the plasma flows to the downstream region. The density for the case B1 was calculated as such at the nozzle from experimentally observed pressure together with conditions of the vacuum system. However, the effect of the helium contact cooling of case B1 is still insufficient. As we increase the value of helium density assumed at $z = 0$, the agreement becomes better. At $z = 1\mathrm{cm}$, numerical results of case B3 agrees best of the three assumed cases. Therefore, it is concluded that the value of helium density just near the nozzle should be about $(1-2) \times 10^{16}\mathrm{cm}^{-3}$.

On the other hand, for the downstream region ($z \geq 8$ cm), the agreement of the case B1 is the worst again, where the effect of gas contact cooling becomes too strong to reproduce the experimental result. In the downstream region, the helium gas density should become lower, at least like the case B2. Nevertheless, the electron temperature calculated for the case B2 is still lower than that measured experimentally. It should be noted that the agreement is not much improved even if we assume lower helium density there. As a matter of fact, the helium density of the case B3 at $z \geq 1$ cm is considered to be unrealistically low, if we consider the conductance of our vacuum system. When we assume that the helium density should be $1 \times 10^{15}\,\mathrm{cm}^{-3}$ (case B2) in this region, the effect of helium contact cooling becomes less remarkable than that by ion-electron collisions. Therefore, the helium density at $z \geq 8$ cm is estimated to be the order of $1 \times 10^{15}\,\mathrm{cm}^{-3}$.

Concerning population densities, it is seen that the present numerical results approximately reproduce the experimental ones. It is confirmed that the present modeling is quantitatively sufficient to simulate the population densities as well as the electron temperature of the argon plasma jet for case A (without gas-contact). For case B, however, disagreement is remarkable, especially, at $z = 8$ cm and 15 cm. This is because the numerical result of the electron temperature, shown in Fig. 5 (b), was much lower than the experimental results for case B2. Of course, the agreement for the He density assumption of case B2 is much more improved than that of the case B1. However, the agreement was not improved even when we assumed the density profile to be that of case B3, where He number density was unrealistically low. It is considered that these disagreement shows the limit of validity of the present numerical model,

where the longitudinal velocity of the plasma jet is constant, and the plasma flow is treated as a one-dimensional problem. In order to improve the numerical simulation, we should understand not only fluid dynamic behavior of helium gas introduced into the plasma chamber but also that of the plasma jet itself, which is beyond the scope of the present study. Further discussion is given elsewhere [13].

CONCLUSION

The experiment of He gas-contact for cooling of electrons in the recombining Ar plasma jet was demonstrated. Without helium gas contact, electron temperature of the Ar plasma decreased slowly, and in consequence, no population inversion was found in excited states of Ar I. By the helium contact cooling, the electron temperature decreased very rapidly as the plasma jet came downstream, and population inversion was created. Population inversion between Ar I excited states of $5s' \rightarrow 4p'[1/2]_1$ and $5s' \rightarrow 4p[3/2]_{1,2}, [5/2]_{2,3}$ occurred through rapid electron cooling by elastic collision between electrons and He atoms. This is attributed to the difference in the electron elastic collision cross section between helium and argon. The electron collision cross section of Ar has its minimum around electron energy $0.2 - 0.5$ eV due to the Ramsauer effect, which is not the case with helium. Therefore, it was confirmed that electron energy was transferred by elastic collisions of electrons to the neutral gas molecules in the recombining plasma jet. In addition to the experiments, numerical calculation was carried out to understand the temporal variation of electron temperature and of population densities of excited states of argon atoms. Consequently, it was found that numerical methods which we previously proposed quantitatively explained the variation of the electron temperature and population densities for the case without helium contact cooling. On the other hand, for the case with gas-contact, three hypothetical He number density profiles were assumed and we confirmed the agreement of electron temperature and number densities of PLTE levels between calculations and experiments. However, the agreement of the population densities of lower lying excited levels in the state of non-PLTE was rather qualitative, due to the simplified modeling of the fluid dynamics of the helium gas introduced into the argon plasma as well as those of plasma jet itself.

ACKNOWLEDGMENTS

The authors thank Professor J. Vlček of the University of West Bohemia for allowing us to use his excellent argon CR model code.

REFERENCES

1. H. Akatsuka and M. Suzuki, Rev. Sci. Instrum. **64**, 1734 (1993).
2. H. Akatsuka and M. Suzuki, Phys. Rev. E **49**, 1534 (1994).
3. H. Akatsuka and M. Suzuki, Contrib. Plasma Phys. **34**, 539 (1994).
4. H. Akatsuka and M. Suzuki, Plasma Sources Sci. Technol. **4**, 125 (1995).
5. T. Fujimoto, J. Phys. Soc. Jpn. **47**, 265, 273 (1979).
6. A. W. Yau, R. P. McEachran, and A. D. Stauffer, J. Phys. B: At. Mol. Opt. Phys. **13**, 377 (1980).
7. K. Kano and H. Akatsuka, Jpn. J. Appl. Phys. **40**, 4701 (2001).
8. J. Vlček, J. Phys. D: Appl. Phys. **22**, 623 (1989).
9. U. Furukane and T. Oda, Z. Naturforsch **39a**, 132 (1984).
10. U. Furukane, K. Sato, and T. Oda, J. Phys. D: Appl. Phys. **22**, 390 (1989).
11. A. Gilardini, *Low Energy Electron Collisions In Gases* (John Wiley & Sons, New York, 1972), (ed. S. C. Brown).
12. Y. Itikawa, Phys. Fluids **16**, 831 (1973).
13. K. Kano and H. Akatsuka, Phys. Rev. E **65**, 056404 (2002).